Effect of Trehalose on the Nonbond Associative Interactions between Small Unilamellar Vesicles and Human Serum Albumin and on the Aging Process

ARTICLE *in* LANGMUIR · OCTOBER 2002

Impact Factor: 4.46 · DOI: 10.1021/la026166q

4 AUTHORS, INCLUDING:

Irén Bárdos-Nagy
Semmelweis University
6 PUBLICATIONS **91** CITATIONS

SEE PROFILE

Judit Fidy
Semmelweis University
127 PUBLICATIONS **1,623** CITATIONS

SEE PROFILE

Effect of Trehalose on the Nonbond Associative Interactions between Small Unilamellar Vesicles and Human Serum Albumin and on the Aging Process

Irén Bárdos-Nagy, Rita Galántai, Monique Laberge, and Judit Fidy*

Semmelweis University, Faculty of Medicine, Department of Biophysics and Radiation Biology, Budapest, Hungary

Received July 1, 2002. In Final Form: September 6, 2002

The effect of trehalose on the interaction of human serum albumin (HSA) with neutral and negatively charged small unilamellar vesicles (SUVs) composed of 1,2-dimyristoyl-*sn*-glycero-3-phosphatidylcholine (DMPC) or of mixtures of DMPC (19:1 w/w) with 1,2-dimyristoyl-*sn*-glycero-3-phosphatidylglycerol (DMPG) was studied by time-resolved fluorescence and dynamic light scattering measurements. The results are interpreted with supporting nonbond calculations describing the nonbond domains most likely to be involved in the protein−SUV interaction. In the absence of trehalose, lifetime measurements of the single Trp of HSA are indicative of two different SUV−HSA associative mechanisms depending on the [lipid]/[HSA] concentration ratios. At low ratios, depletion of phospholipid molecules from vesicles by HSA occurs independently of the lipid composition of the vesicles via favorable hydrophobic contacts. At higher ratios, vesicle−HSA assocation is favored by electrostatic interactions for the negatively charged SUVs. For neutral SUVs, hydrophobically driven penetration of HSA is proposed. All association mechanisms are damped in the presence of trehalose, due to its capacity to coat the interacting surfaces. The results of dynamic light scattering experiments clearly show that the aging of the liposomes is dependent on the lipid composition. The aging of DMPC vesicles is faster and not affected by the presence of either HSA or trehalose. The aging of DMPC/DMPG liposomes is more pronounced in the presence of HSA. These SUVs are stabilized by trehalose through different mechanisms depending on whether they are covered by HSA or not.

Introduction

The stabilizing effect of trehalose on membranes and on a variety of macromolecules is now firmly established.[1] The disaccharide is also known as a very efficient cryoprotectant, preventing fusion and aggregation in lipid membranes and reducing leakage of material enclosed in vesicles or membranes during dehydration.[2−7] As such, trehalose is commonly used by the pharmaceutical industry to increase the stability of liposome systems. This action of trehalose has been attributed to its hydrogen bonding capacity, its glass characteristics, its ability to modify the lipid solvation layer, and its large hydrated volume when compared to those of other carbohydrates (e.g. 2.5 times that of sucrose).[8−10] Specifically, when lipid bilayers are hydrated, two hydration layers form and it has been suggested that the first layer of water molecules at the lipid−water interface makes a major contribution to the dipole potential of the membrane, known to arise from the functional group dipoles of the terminal methyl groups, the glycerol−ester lipid regions, and polar headgroups.[11] This first layer is polarized, whereas the second is disordered, and is also hydrogen-bonded to lipid headgroups.[12,13] Unlike other sugars, trehalose has been shown to decrease the dipole potential because it can bind to lipid carbonyl groups and displace polarized waters in the first hydration layer.[14] In previous work, we used fluorescence intensity and anisotropy measurements to examine how the presence of trehalose, in a concentration suitable for rehydration of freeze-dried liposomes, influences the interaction of porphyrins with small unilamellar vesicles (SUVs) and human serum albumin (HSA).[15] Our interpretation was that low concentrations of trehalose were able to interact with the lipid headgroups and that the effect was enhanced in SUVs of anionic character. Trehalose affected the location of the porphyrins within the SUVs, and we suggested that it hindered the binding of HSA to the liposome surface.

In this work, we use time-resolved fluorescence lifetime measurements of Trp 214, the single Trp residue of HSA (Figure 1), and a combination of electrostatic and hydrophobic calculations on HSA to describe its nonbond properties. Our experiments investigate the SUV−HSA, SUV−trehalose, and SUV−HSA−trehalose interactions

* To whom correspondence should be adressed. E-mail: judit@puskin.sote.hu. Phone: 36-1-267-6261. Fax: 36-1-266-6656. Mailing address: P.O. Box 263, Budapest H-1444, Hungary.

(1) Sola-Penna, M.; Meyer-Fernandez, J. R. *Arch. Biochem. Biophys.* **1998**, *360*, 10−14.
(2) Crowe, J. H.; Crowe, L. M.; Chapman, D. *Science* **1984**, *223*, 701−703.
(3) Fabrie, C. H. J.; de Kruijff, P. B.; de Gier, J. *Biochim. Biophys. Acta* **1990**, *1024*, 380−384.
(4) Tsvetkova, N. M.; Phillips, B. L.; Crowe, L. M.; Crowe, J. H.; Risbud, S. H. *Biophys. J.* **1998**, *75*, 2947−2955.
(5) Crowe, J. H.; Crowe, L. M.; Carpenter, J. F.; Wistrom, C. A. *Biochem. J.* **1987**, *242*, 1−10.
(6) Clegg, J. S.; Seitz, P.; Seitz, W.; Hazlewood, C. F. *Cryobiology* **1982**, *19*, 306−316.
(7) Harrigan, P. R.; Madden, T. D.; Cullis, P. R. *Chem. Phys. Lipids* **1990**, *52*, 139−149.
(8) Crowe, J. H.; Carpenter, J. F.; Crowe, L. M. *Annu. Rev. Physiol.* **1998**, *60* 73−103.
(9) Sano, F.; Asakawa, N.; Inoue, Y.; Sakurai, M. *Cryobiology* **1999**, *39*, 80−87.
(10) Xie, G.; Timasheff, S. N. *Biophys. Chem.* **1997**, *64*, 25−43.
(11) Essman, U.; Perera, L.; Berkowitz, M. *Langmuir* **1995**, *11*, 4519−4531.
(12) Brockman, H. *Chem. Phys. Lipids* **1994**, *73*, 57−79.
(13) Diaz, S.; Amalfa, F.; Biodi de Lopez, A. C.; Disalvo, E. A. *Langmuir* **1999**, *15*, 5179−5182.
(14) Luzardo, M. C.; Amalfa, F.; Nunez, A. M.; Diaz, S.; Biondi De Lopez, A. C.; Disalvo, E. A. *Biophys. J.* **2000**, *78*, 2452−2458.
(15) Bárdos-Nagy, I.; Galántai, R.; Fidy, J. *Biochim. Biophys. Acta* **2001**, *1512*, 125−134.

10.1021/la026166q CCC: $25.00
Published on Web 10/25/2002

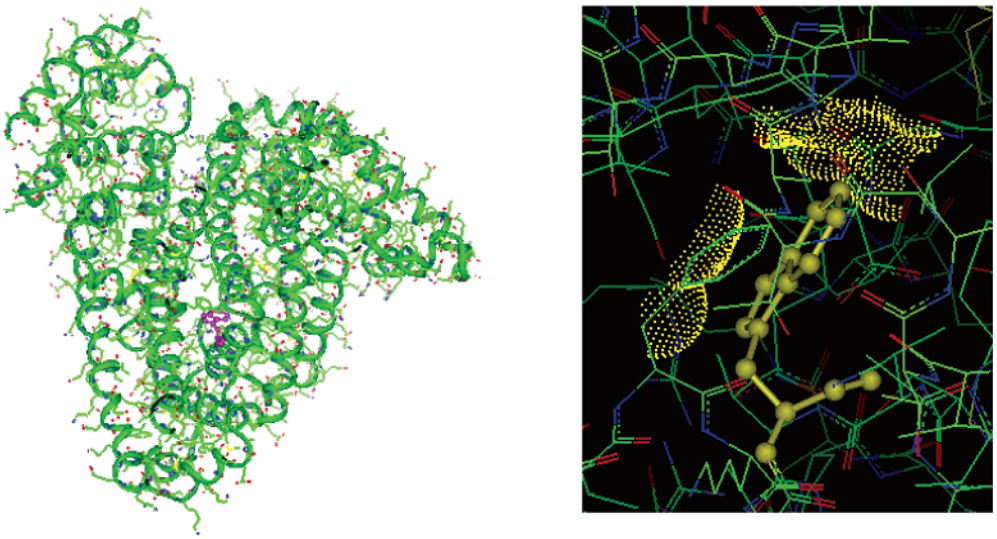

Figure 1. Right: ribbon rendering of HSA showing its single Trp residue as a purple stick rendering. Left: detail of the Trp residue with the Connoly surface rendered as yellow dots. SASA ratio: 23.4.

and their dependence on the lipid composition of liposomes, consisting either of 1,2-dimyristoyl-*sn*-glycero-3-phosphatidylcholine (DMPC) or of mixtures (19/1 w/w) of DMPC with 1,2-dimyristoyl-*sn*-glycero-3-phosphatidylglycerol (DMPG). The headgroup of DMPC has a positively charged choline group and a negatively charged phosphate and a polar carbonyl group, but DMPC as a whole achieves charge neutrality. The addition of DMPG, lacking the positive choline group, to the DMPC liposomes thus provides negative charge to the SUVs. We used dynamic light scattering measurements to determine the size of the SUVs and to study the effect of trehalose on the aging of the liposome and liposome−HSA systems.

Methods Section

Experimental Methods. *Chemicals.* DMPC, DMPG, lyophilized HSA, and α−α trehalose were purchased from Sigma. The lipids were crystallized one time. The solvents (chloroform, methanol) were obtained from Merck. All chemicals were of spectroscopic grade.

Preparation of HSA Solutions and Liposomes. The purification of HSA and the preparation of sonicated SUVs consisting of DMPC and DMPC/DMPG (19/1 w/w) in 10^{-2} M sodium phosphate buffer at pH 7.4 are fully described elsewhere.[16,17] The concentration of HSA was determined using $\epsilon_{280} = 37\,400\ M^{-1}\ cm^{-1}$ in phosphate buffer. When trehalose was used, the lipids were hydrated using the same phosphate buffer with 3×10^{-2} M trehalose. This sugar concentration is relatively low but falls into the concentration range typical of trehalose-treated and freeze-dried/rehydrated liposome solutions.[18] In all experiments, the same trehalose concentration was used.

Fluorescence Lifetime Measurements. Lifetimes were measured using a CD900 luminometer equipped with a F900 40 kHz ns flash-lamp (Edinburgh Analytical Instruments Edinburgh, U.K.). Fluorescence decay curves were acquired using a time-correlated single-photon counting technique, and the lifetimes were analyzed with the FL900CDA software package (Edinburgh Analytical Instruments) using a reconvolution method. The full width at half-maximum (fwhm) value of the lamp function was ∼1.5 ns. The temperature of the sample was kept at 32 °C in all experiments.

Dynamic Light Scattering Measurements. The measurements were performed using an ALV goniometer with a 35 mW He−Ne laser ($\lambda = 632.8$ nm) light source. Particle size distributions were determined by acquiring correlation time functions using the maximum entropy method.[19]

Computational Methods. *Modeling the HSA Structure.* The X-ray coordinates of the 2.5 Å-resolution structure of dimeric HSA (1AO6.pdb)[20] were obtained from the RCSB repository[21] and prepared for nonbond calculations using the *InsightII* software package, version I2000 (Accelerys Inc., San Diego). The c27b1 version of CHARMM[22] was used for energy minimization, and the CVFF force field, for the hydropathic interaction (HINT) calculations (vide infra). A HSA monomer was extracted from the pdb coordinates, as the protein exists in monomeric form under our experimental conditions. Explicit hydrogens were added, consistent with pH 7.0 using HBUILD for a total of 9121 atoms; the N- and C-termini were modeled as NH_3^+ and COO^-. The HSA model was then subjected to extensive minimization so as to optimize the structure prior to the nonbond interaction calculations. All hydrogens were first subjected to 50 steps of steepest descent minimization while constraining the heavy atoms. The system was then subjected to 10 conjugate gradient minimization cycles of 100 steps each, progressively decreasing harmonic constraints from 400 to 5 $kcal^{-1}$ mol A^{-2}, followed by 20 000 steps of Adopted Basis Newton Raphson minimization. The SHAKE algorithm was used for the first minimization cycles, and the second minimization cycle was performed on a parallel supercomputing environment. To distinguish between unfavorable polar−polar interactions that would be screened by solvent and those which would not, the HSA system was also solvated in a 2 Å-layer of solvent (2582 water molecules) and a new set of calculations was performed. The solvent accessible surface areas (SASAs) of residues were calculated using the program FANTOM/GETAREA.[23] This program uses a 1.4 Å-probe and reports SASAs as ratios of side-chain surface area to random coil value per residue, which is the average SASA of the residue in the tripeptide Gly-X-Gly in an ensemble of 30 random conformations. Residues are considered exposed to solvent if *R* exceeds 50% and buried if *R* is less than 20%.

Calculation of HSA Nonbond Interactions. Hydrophobic and polar interactions were calculated using the HINT program

(16) Galántai, R.; Bárdos-Nagy, I.; Módos, K.; Kardos, J.; Závodszky, P.; Fidy, J. *Arch. Biochem. Biophys.* **2000**, *373*, 261−270.
(17) Galántai, R.; Bárdos-Nagy, I. *Int. J. Pharm.* **2000**, *195*, 207−218.
(18) Womersley, C.; Uster, P. S.; Rudolph, A. S.; Crowe, J. H. *Cryobiology* **1986**, *23*, 245−255.
(19) Bryan, R. K. In *Maximum entropy and Bayesian Methods*; Fougere, P. F., Ed.; Kluver Academic Publishers: Dordrecht, The Nederlands, 1990; pp 221−232.
(20) Sugio, S.; Kashima, A.; Mochizuki, S.; Noda, M.; Kabayashi, K. *Protein Eng.* **1999**, *12*, 439−446.
(21) Bernstein, F. C.; Koetzle, T. F.; Williams, G. J.; Meyer, B. E. F., Jr.; Brice, M. D.; Rodgers, J. R.; Kennard, O.; Shimanouchi, T.; Tasumi, M. *Eur. J. Biochem.* **1977**, *80*, 319−324.
(22) Brooks, B. R.; Bruccoleri, R. E.; Olafson, B. D.; States, D. J.; Swaminathan, S.; Karplus, M. *J. Comput. Chem.* **1983**, *4*, 187−217.
(23) Fraczkiewicz, R.; Braun, W. *J. Comput. Chem.* **1998**, *19*, 319−333.

developed by Kellogg and Abraham.[24] HINT is designed to calculate and map the nonbond environment of proteins. It uses experimental solvent partitioning data as a basis for an empirical molecular interaction model. The fundamental quantity calculated by the program is the "hydrophobic atom constant", which contains implicit contributions from bond, chain, and polar proximity factors. These values are calculated following the fragment constant method of Rekker, Leo, and Hansch[25,26] adapted for protein systems. The advantage of the method is that the partition coefficient (log *P*, the sum of the hydrophobic atom constants) is a thermodynamic experimental parameter. As such, it is unbiased and provides interaction information specific to the biological environment and entropy of the system. HINT generates lists of specific atom−atom interactions and molecular grid maps that show the detail of the calculated interactions. The hydrophobic field is calculated by superposing a grid of points in space around the atoms of interest and calculating the net sum at each test point according to[24]

$$A_p = \sum_{i=1} s_i a_i R_{ip} \qquad (1)$$

where s_i is the SASA and a_i the hydrophobic atom constant of the ith atom. R_{ip} is the distance function that controls the mathematical form of the distance (r) dependence for the calculated interactions between the ith atom and the grid point p; in this case, $R_{ip} = e^{-r(ip)}$. The calculations were performed with version 2.35 (EduSoft LC, Ashland, VA), interfaced to *InsightII*. The spacing between grid points was 0.5 Å. Two calculations were performed over the grid at a cutoff radius of 8 Å: (i) calculation of hydrophobic interactions, in which all hydrophobic−hydrophobic interactions were recorded as positive contributions and all hydrophobic−polar contributions as negative ones; (ii) calculation of polar−polar interactions, in which all energetically favorable interactions were recorded as positive and all unfavorable interactions as negative.

HSA Electrostatic Calculations. Electrostatic potential maps were calculated for HSA. These maps were generated using the Grasp software package, which creates molecular surface maps using a Poisson−Boltzmann solver, essentially a graphical version of the finite difference solutions to the PB equation which are implemented in the Delphi software package.[27,28] Electrostatic parameters were set as follows: $\epsilon_{inner} = 2.0$; $\epsilon_{outer} = 79.0$; water probe radius = 1.4 Å; ionic radius = 2.0 Å; salt concentration = 0.010 M, reflecting the experimental conditions. All calculations were performed using the PARSE charge set[29] with titratable residues corresponding to their neutral pH charge. The electrostatic potential is calculated using the FDPB solver implemented in Grasp, which is then used to color-code the generated surfaces (negative potential is red and positive blue).

Results

Effect of Liposomes on the Trp Fluorescence Decay in the Absence and in the Presence of Trehalose. HSA has only one Trp residue with a SASA ratio of 23.4 (Figure 1), and as such, it is a good candidate to report on its local surroundings. The position of its maximum emission is not shifted by the presence of either type of SUV and by trehalose. Figure 2, however, shows a pronounced effect of the presence of the DMPC or DMPC/DMPG SUVs on the Trp lifetime measured as a function of the [lipid]/[HSA] ratio (filled symbols). The fluorescence decay curves could be satisfactorily fitted to two components. The longer component was used to plot the data in Figure 2. To facilitate comparison, we plotted the percent change of the lifetimes relative to the Trp lifetime measured in a solution containing only HSA.

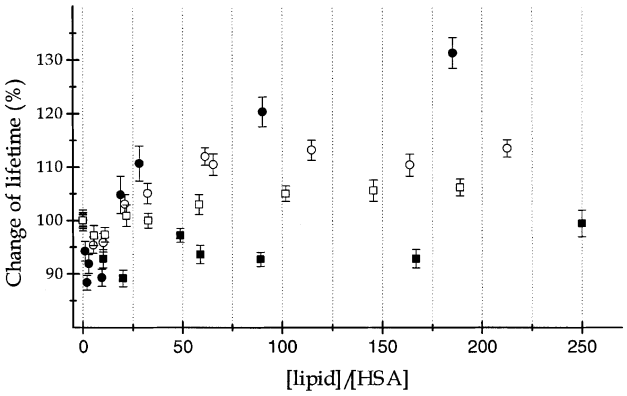

Figure 2. Effect of DMPC (squares) and DMPC/DMPG (circles) liposomes on the longer component of the Trp fluorescence lifetime recorded in a 5×10^{-6} M HSA solution in the absence (filled symbols) and in the presence (unfilled symbols) of 3×10^{-2} M trehalose.

Two regimes are clearly distinct: (i) an initial quenching of the lifetimes at [lipid]/[HSA] ratios lower than ∼15. This effect is observed for both types of SUVs. (ii) At lipid ratios > ∼15, the lifetimes start increasing. In the case of DMPC, the lifetimes are close to that measured in the absence of liposomes. The strongest increase in Trp lifetimes occurs in the presence of DMPC/DMPG liposomes: at a [lipid]/[HSA] ratio of 180, the lifetime increases by more than 30%.

Both the quenching (at low lipid concentration) and the increase (at high lipid concentration) of the Trp lifetime are strongly affected by trehalose (Figure 2, unfilled symbols). The presence of the disaccharide alleviates the quenching of the Trp lifetimes for both types of liposomes at low lipid concentrations. Similarly, at higher lipid concentrations, the effect of trehalose on the lifetimes minimizes the significant difference observed between the DMPC and the DMPC/DMPG liposomes in its absence. Control measurements on a trehalose−HSA solution verified that the disaccharide alone has no effect on the Trp lifetime.

Size Distribution of Liposomes in the Absence and in the Presence of HSA and Trehalose. Dynamic light scattering experiments were performed to compare the DMPC and DMPC/DMPG liposomes prepared for the lifetime measurements. The size distribution of the vesicles was determined in the absence and in the presence of trehalose in liposome (DMPC, DMPC/DMPG) and liposome−HSA (DMPC−HSA and DMPC/DMPG−HSA) solutions.

The measurements were performed on freshly prepared liposome solutions (10^{-3} M lipid concentration) and on the liposome−HSA system at a 0.01 [HSA]/[lipid] concentration ratio after 30 min of incubation. Calculated on the basis of the molecular size of HSA and the average diameter of liposomes, this HSA ratio is large enough to cover the total surface of liposomes.[17]

The distribution curves shown in Figure 3 as full lines compare the effect of HSA and trehalose on the size distribution of the freshly prepared DMPC/DMPG SUVs. Their average radius was ∼14−16 nm (Figure 3A, full line). The DMPC SUV's were of the same average size (data not shown). However, their distribution function was somewhat broader than that of the DMPC/DMPG vesicles. The presence of HSA (Figure 3B) increases the average size of the freshly prepared DMPC/DMPG lipo-

(24) Meng, E. C.; Kuntz, T. D.; Abraham, D. J.; Kellogg, G. E. *J. Comput.-Aided Mol. Des.* **1994**, *8*, 299−306.
(25) Rekker, R. F. *The Hydrophobic Fragmental Constant: Its Derivation and Application*; Elsevier Science: Amsterdam, 1977.
(26) Hansch, C.; Leo, A. J. *Substituent Constants for Correlation Analysis in Chemistry and Biology*; J. Wiley & Sons: New York, 1979.
(27) Jayaram, B.; Sharp, K. A.; Honig, B. *Biopolymers* **1989**, *28*, 975−993.
(28) Nicholls, A.; Honig, B. *J. Comput. Chem.* **1991**, *12*, 435−445.
(29) Sitkoff, D. K.; Sharp, K. A.; Honig, B. *J. Phys. Chem.* **1994**, *98*, 1978−1988.

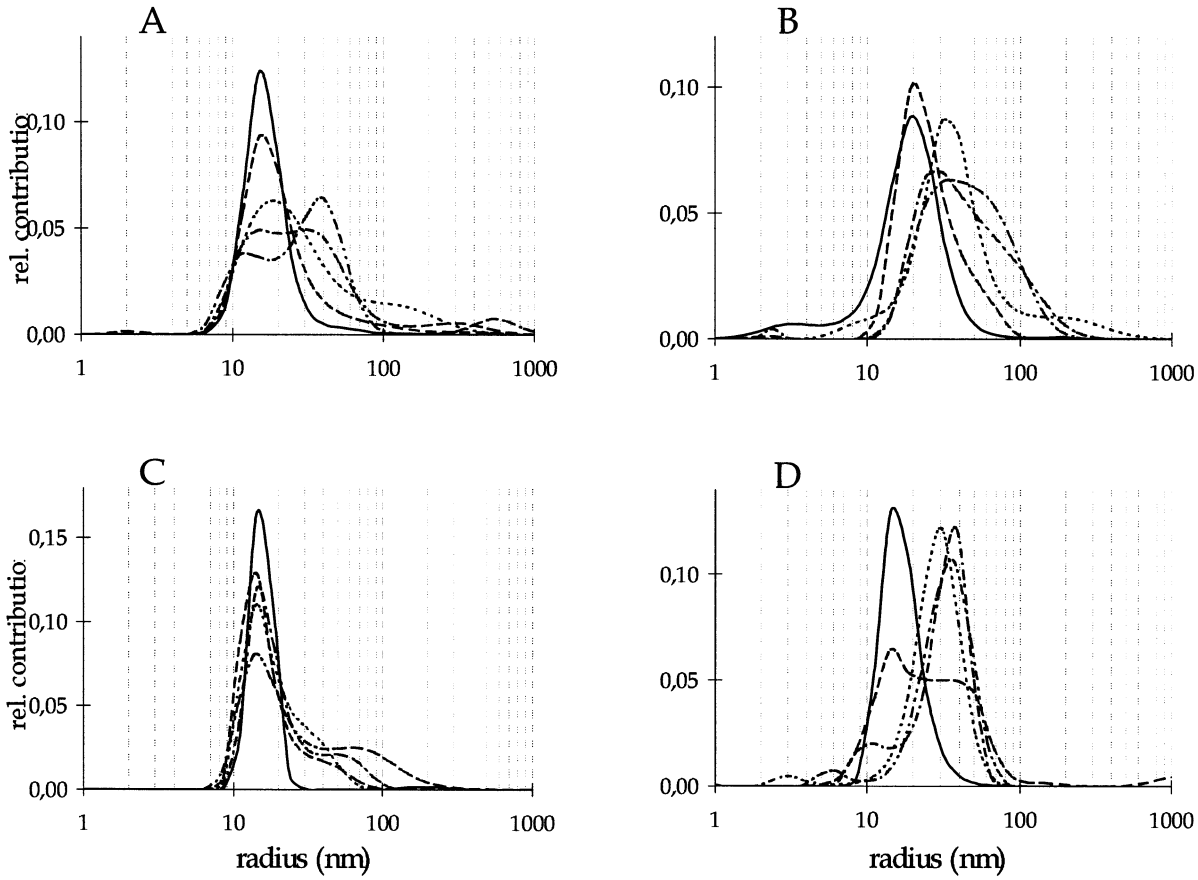

Figure 3. Effect of HSA and trehalose on the size distribution of DMPC/DMPG liposomes as a function of time (A) in liposome (at 10^{-3} M lipid concentration), (B) in liposome−HSA (at 0.01 [HSA]/[lipid] concentration ratio), (C) in liposome−trehalose (at 3 $\times$ 10^{-2} M trehalose concentration), (D) in liposome−HSA-trehalose solutions. The curves represent the relative contribution of liposomes to the correlation function of light scattering as a function of size: for the freshly prepared (solid) and the 3 day (dash), 5 day (dot), 8 day (dash−dot), and 10 day (dash−double dot) old liposome solutions.

somes by ~5 nm and also broadens the distribution curve, with no significant difference observed with the DMPC SUVs. The presence of trehalose is seen to narrow the distribution functions of the liposomes alone (Figure 3C) as well as that of the liposomes in the presence of HSA (Figure 3D). This narrowing effect of the sugar was not observed with the DMPC vesicles.

Effect of Trehalose on the Aging of Liposomes. The aggregation and fusion of liposomes is highly dependent on the environment. The interaction between the liposomes and HSA or trehalose may also modify the size distribution during the aging process of the liposomes. To investigate the influence of HSA and trehalose on the stability of the SUVs, the dynamic light scattering experiments were also performed as a function of time, namely every day during a 10-day period.

The neutral liposomes had a wider distribution curve, and their increase in size was more pronounced in time (data not shown). After 4 days, the average radius of the DMPC vesicles was larger than 50 nm. Similar to the case of the size distribution of the fresh liposomes, the aging process was not significantly influenced by HSA or by trehalose in the case of the DMPC vesicles.

The size distribution of DMPC/DMPG liposomes as a function of time is shown in Figure 3A. As the liposomes are getting older, their size increases: the maximum of the distribution function is shifted to the direction of larger radii, the initial peak decreases, and a new peak with a ~2.5 times larger radius (~40 nm) appears. This aging process is significantly affected by HSA (Figure 3B) and by trehalose alone (Figure 3C) and also by both components combined (Figure 3D). The aging of the liposome−HSA system does not result in a definite particle size; rather, the radius of the particles continuously increases in time. The maximum of the distribution function is shifted toward the larger radii, and the width of the population broadens as a function of time.

The effect of trehalose on the size distribution and aging of DMPC/DMPG liposomes is different in the absence and in the presence of HSA (Figure 3C and D, respectively). In the absence of HSA, the initially existing smaller liposomes are stabilized by trehalose. The liposome population is more definite; the width of the distribution curve is narrower. The conversion of this distribution to bigger vesicles is hindered: the appearance of a new population requires longer time compared to that for the system without trehalose (Figure 3A).

In the presence of HSA, another effect can be observed (Figure 3D). In the DMPC/DMPG liposome−trehalose−HSA system, the average size of the particles in the freshly prepared solution is the same as that in the liposome solutions in the absence (Figure 3A) and in the presence of trehalose (Figure 3C). This distribution, however, totally and relatively quickly (4−5 days) rearranges into a new one with a definite size and width. The further time evolution does not significantly influence the size distribution of this system.

Calculation of HSA Nonbond Interactions. Table 1 presents the SASA ratios calculated for HSA. Out of 578 residues, 173 are exposed to solvent, 56% being polar residues with charged side-chains, namely 40 Glu residues, 21 Asp, 33 Lys, and 3 Arg. Figure 4 shows the interaction

Table 1. Solvent Accessible Surface Areas of the HSA Residues

residue	*R* (%)	residue	*R* (%)	residue	*R* (%)	residue	*R* (%)
His 9	50.4	Ala 163	84.7	Lys 317	78.8	Thr 474	54.4
Lys 12	59.5	Thr 166	61.1	Asn 318	65.4	Lys 475	59.9
Glu 17	96.3	Glu 167	66.4	Ala 320	79.3	Thr 478	76.9
Pro 35	50.1	Gln 170	82.2	Glu 321	60.4	Glu 479	68.5
Glu 37	77.0	Ala 172	100.0	Ala 322	65.0	Asn 483	52.5
Asn 44	54.5	Asp 173	71.7	Lys 323	56.5	Ala 490	87.2
Glu 48	84.8	Ala 175	75.5	Asp 324	54.0	Glu 492	85.7
Lys 51	52.4	Ala 176	66.8	Val 325	67.3	Glu 495	83.0
Thr 52	63.3	Pro 180	62.3	Lys 351	64.4	Thr 496	90.5
Ala 55	83.4	Glu 184	75.8	Thr 355	58.1	Val 498	98.7
Asp 56	56.5	Asp 187	62.6	Glu 358	56.5	Lys 500	89.9
Glu 57	52.9	Lys 195	53.5	Lys 359	80.4	Glu 501	92.0
Ser 58	89.2	Lys 205	60.1	Ala 362	86.6	Ala 504	100.0
Asp 63	84.2	Glu 208	63.3	Ala 364	100.0	Glu 505	97.2
Ser 65	71.2	Arg 209	62.3	Asp 365	78.4	Thr 506	57.0
Asp 72	54.6	Glu 227	83.8	His 367	50.6	His 510	74.7
Thr 79	61.7	Ala 229	93.5	Glu 368	98.2	Asp 512	74.8
Arg 81	80.5	Thr 236	69.5	Ala 371	55.4	Thr 515	75.8
Glu 82	100.0	Lys 240	64.4	Lys 372	73.4	Glu 518	59.4
Glu 86	88.9	Thr 243	52.7	Asp 375	68.3	Lys 519	75.3
Asp 89	82.9	Asp 259	69.5	Glu 376	55.8	Lys 524	57.8
Ala 92	74.6	Lys 262	68.8	Lys 378	74.1	Lys 538	96.9
Gln 94	93.8	Glu 266	62.5	Pro 379	77.6	Ala 539	87.9
Pro 96	92.6	Asp 269	95.5	Glu 382	62.4	Lys 541	90.4
Glu 97	61.0	Ser 270	63.5	Asn 386	63.9	Glu 542	92.5
Glu 100	68.6	Ser 273	70.1	Lys 389	72.7	Lys 545	56.7
Gln 104	69.5	Lys 276	71.8	Gln 390	72.9	Ala 546	72.0
Asn 109	57.4	Glu 277	73.8	Glu 393	68.1	Asp 549	72.3
Asn 111	79.4	Glu 280	75.1	Glu 396	67.2	Ala 553	64.0
Pro 113	88.0	Pro 282	71.2	Gln 397	57.6	Glu 556	60.8
Arg 114	81.7	Leu 283	53.7	Lys 402	66.3	Lys 557	65.2
Leu 115	54.7	Glu 292	51.6	Ser 419	60.8	Lys 560	84.5
Val 116	88.9	Glu 294	82.8	Pro 421	82.4	Asp 562	93.3
Glu 119	77.9	Glu 297	74.5	Lys 436	50.0	Lys 564	96.5
Asp 121	70.9	Ala 300	100.0	Lys 439	96.0	Glu 565	84.1
Thr 125	84.0	Asp 301	98.9	Pro 441	70.8	Thr 566	61.4
Ala 126	55.5	Pro 303	65.9	Glu 442	98.1	Ala 569	62.9
His 128	52.2	Ser 304	87.1	Ala 443	75.8	Glu 570	67.5
Asp 129	80.1	Ala 307	63.9	Lys 444	61.4	Lys 573	76.7
Asn 130	54.8	Asp 308	65.0	Glu 465	54.6	Lys 574	87.9
Glu 132	80.2	Glu 311	67.1	Thr 467	80.1	Ala 577	76.9
Thr 133	57.7	Lys 313	85.7	Pro 468	73.8	Ala 578	68.2
Lys 137	55.6	Asp 314	65.0	Asp 471	100.0	Gln 580	58.1
						Ala 581	81.5

map generated by HINT for the entire HSA structure. The contour surfaces overwhelmingly indicate the predominance of favorable polar−polar surface interactions (blue regions), consisting of H-bonding, electrostatic, and charge−charge interactions. Examining the favorable hydrophobic−hydrophobic interactions (green regions) from the numerical data sets yields four buried clusters where this type of interaction strongly predominates and two additional minor zones (cf. Table 2). Figure 5 illustrates one such hydrophobic cluster. Most of the residues involved in this type of interactions are well buried in the protein interior with SASA ratios < 20%. Figure 6 shows the Grasp-generated electrostatic potential maps of the molecular surface of HSA in two orientations. The surface of HSA is characterized by a distribution of polar residues (cf. Table 1) with no apparent charge clustering when considering the residue distribution on the surface. However, the calculation of the electrostatic potential ($\Sigma q\Phi$) and mapping of this property onto the molecular surface reveals regions of localized potential density.

Discussion

HSA−liposome Interactions Monitored by the Trp Lifetime Measurements in the Absence of Trehalose. The changes observed in the Trp lifetime as a function of lipid concentration (Figure 2) provide evidence for HSA−liposome interaction. We discuss first the regime

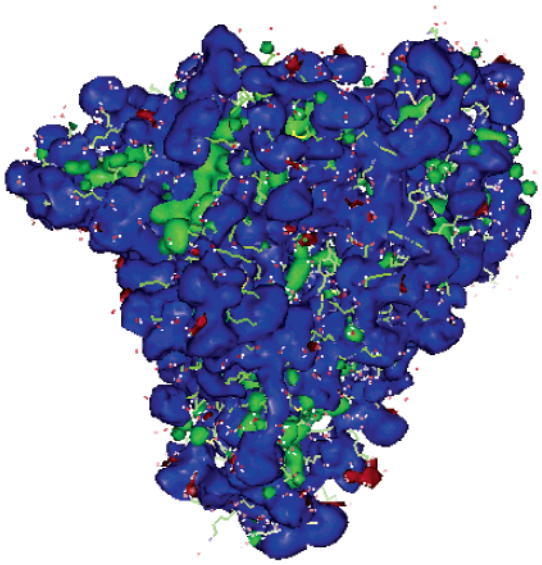

Figure 4. HINT interaction map for HSA generated for the structure with the 2 Å-solvation layer. Blue contours represent favorable polar−polar interactions that include H-bonding, electrostatic, and charge−charge interactions. Red contours represent unfavorable polar−polar interactions (acid−acid, base−base), and green contours represent favorable hydrophobic−hydrophobic contacts. The protein residues are rendered as green lines.

Table 2. Zones of Favorable Hydrophobic Interaction in HSA

zone	residue	SASA (R)	zone	residue	SASA (R)
1	Met 123	14.5	2	Phe 509	4.1
	Ala 126	55.5		Phe 568	0.9
	Phe 165	0.0		Phe 554	0.2
	Phe 127	1.1		Phe 537	9.8
	Phe 149	0.5		Phe 550	0.3
	Phe 134	10.9		Phe 502	17.9
3	Phe 377	2.0	4	Ala 261	2.5
	Phe 374	33.1		Val 293	8.4
	Phe 309	5.5		Leu 260	7.8
	Phe 326	5.6		Leu 275	0.0
	Phe 330	0.1		Phe 223	1.2
	Ile 271	0.0		Ile 290	8.5
				Ile 264	6.7

of lifetime quenching observed at low [lipid]/[HSA] ratio (< ∼15). Considering that a liposome, with a diameter of some ∼50 nm, consists of more than 20 000 phospholipid molecules, the concentration of the vesicles in our systems (10^{-3} M lipid) falls into the 10^{-8} M order of magnitude. Thus, at low [lipid]/[HSA] ratios (< ∼15), the HSA molecules are in large excess and capable of depleting the liposomes of individual phospholipid molecules. We propose that the ensuing monodisperse DMPC and/or DMPG molecules bind HSA through their miristyl chains. Binding to HSA via the fatty acid end is supported by the fact that the change of the Trp lifetime at low lipid concentration is independent of the lipid composition of the liposomes. Additional support is provided by our calculations. Figure 7 shows the hydropathic map of the myristic acid binding site in the HSA−myristic acid complex. The map was generated using the coordinates of the available X-ray structure (1BJ5.pdb).[30] The contour surfaces are color-coded by interaction type, and the volume of the plotted surfaces correlates with the magnitude of the interactions calculated with HINT: green surfaces represent regions of favorable hydrophobic−hydrophobic contacts, and blue

(30) Curry, S.; Mandelkow, H.; Brick, P.; Franks, N. *Nature* **1998**, *5*, 827−834.

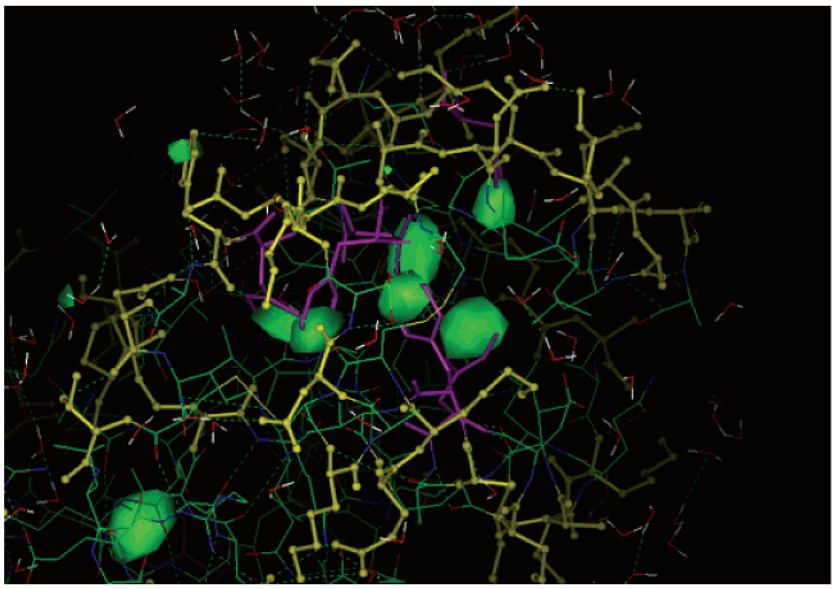

Figure 5. Localized hydrophobic cluster with maximum favorable hydrophobic−hydrophobic interactions shown in green. The residues involved (zone 2 in Table 2) are rendered as purple sticks. Residues colored yellow are solvent-exposed (cf. Table 1).

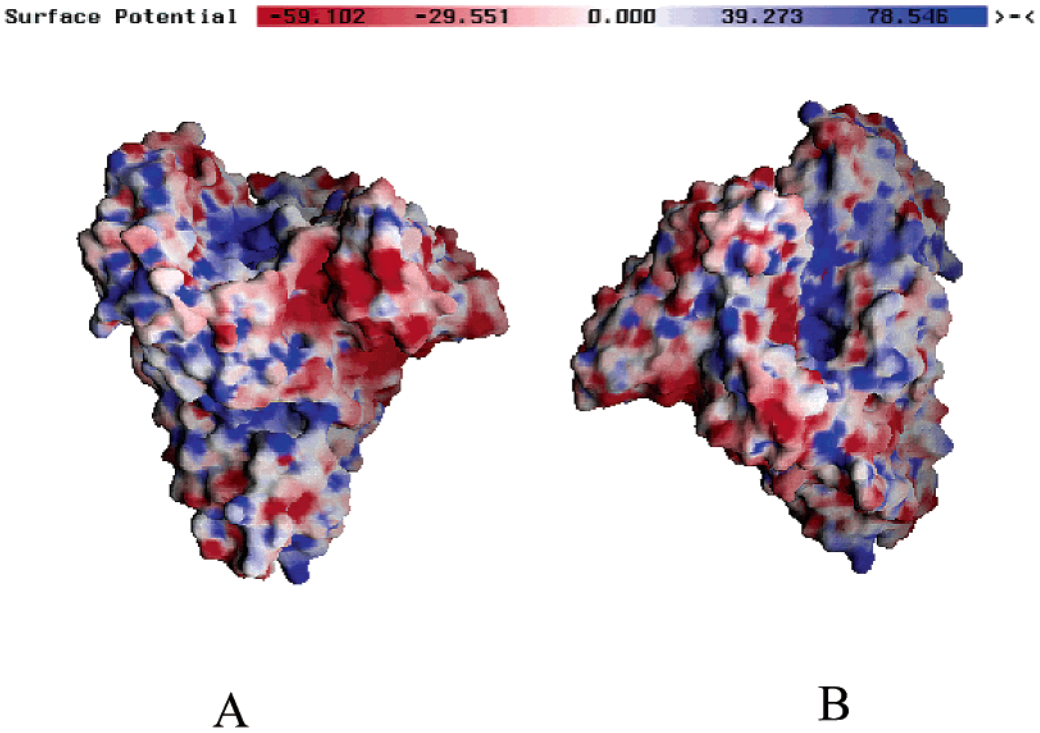

Figure 6. Grasp electrostatic molecular surfaces of HSA. The electrostatic potential is mapped onto the surface and color-coded. Regions of positive potential are blue, and negative regions are red. Three regions of localized positive potential are distinct on one face (A), and one major positive region is distinct on the other face (B). The Trp spectral probe is located in one of the positive potential regions (cf. Figure 1).

surfaces represent favorable polar−polar contacts. The map shows that the alkane chain, completely inserted into the protein matrix, is stabilized by favorable hydrophobic interaction. The binding of myristic acid is also accompanied by a significant conformational change, resulting in a backbone rmsd of 4.61 Å. We suggest that a similar conformational change occurs as a result of HSA binding the single lipid molecules extracted from the SUVs and that it repositions Trp so as to bring it into closer contact with quenchers. Among the well-known Trp quenchers are the peptide bond, the side-chains of Lys, Gln, Asn, His, and Tyr, and the neutral carboxyl group of Glu and Asp.[31,32] In the vicinity of Trp, we find the following potential quenchers: Asp 451 and Lys 199, respectively, at 6.54 and 6.15 Å from Trp, which is also located from 4.06 to ∼6 Å to the closest peptide bonds. The removal of phospholipid molecules from liposomes by HSA is also in agreement with the results obtained with the phosphatidylcholine liposomes−bovine serum albumin system, clearly showing formation of a BSA−phospholipid complex[33] and the recent description of HSA binding sites

(31) Chen, Y.; Barkley, M. D. *Biochemistry* **1998**, *37*, 9976−9982.
(32) Chen, Y.; Liu, B.; Yu, H.-T.; Barkley, M. D. *J. Am. Chem. Soc.* **1996**, *118*, 9271−9278.

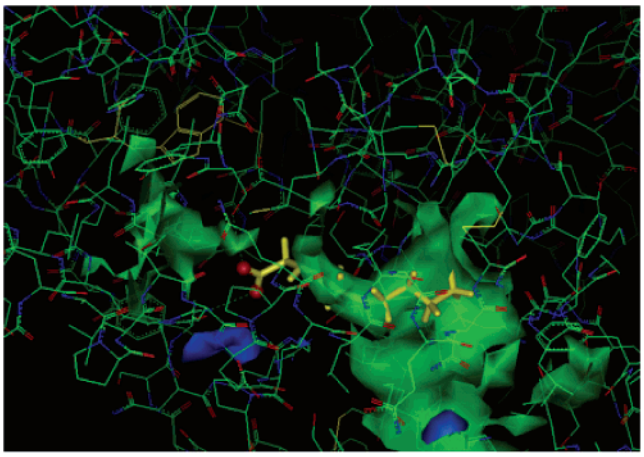

Figure 7. Overlap of favorable hydrophobic−hydrophobic contacts surrounding the fatty acid chain of myristic acid (yellow stick rendering) bound to HSA from the X-ray structure of the myristic acid/HSA complex.[30]

for DMPC-containing liposomes.[34] Depletion of lipid molecules from the red blood cell membrane by serum albumin has also been reported.[35]

At larger [lipid]/[HSA] ratios (> ∼15), we propose that the probability of single lipid molecule removal by HSA becomes negligible and that, under these conditions, the HSA molecules bind to the surface of the liposomes. The overwhelming predominance of favorable polar−polar interactions on the HSA surface (cf. Figure 4) shows that the binding could indeed be driven by such interactions. Inspection of Figure 6 explains the more pronounced effect observed on the Trp lifetimes in the presence of the negatively charged DMPC/DMPG SUVs: the HSA molecular surface shows that there are three regions of localized and uniform positive potential, one on top of the surface shown in the figure (A) and another on the side of the surface (B). The third occurs where Trp 214 located, as can be seen by comparing the location of Trp in Figure 1 and its corresponding electrostatic molecular surface in Figure 6. Calculation of the Trp electrostatic molecular surface alone (not shown) also shows a predominantly positive surface. Thus, the spectral probe is more likely to be affected by the binding of a negatively charged species, which is what we observe experimentally. As for the DMPC binding, not favored by either positive or negative potential regions of HSA since DMPC is overall neutral, it would be expected to be much weaker, which is again what we observe, in agreement with our earlier calorimetric measurements on the same system.[16] The second possibility is that DMPC binding does not occur via electrostatic interactions. Our calorimetric observations had also provided evidence for the penetration of HSA into the vesicles, and our calculations suggest a possible contribution of HSA's hydrophobic clusters (cf. Figure 4, Table 2) to the penetration mechanism: binding in this case would occur via favorable hydrophobic−hydrophobic contacts between the fatty acid intramembrane layer and the hydrophobic zones of the protein and would also result in significant damping of the fluorescence signal, an interpretation supported by the correlation established between hydrophobic clusters on protein surfaces and the binding sites of their cofactors.[36]

HSA−Liposome Interactions Monitored by the Trp Lifetime Measurements in the Presence of Trehalose. The different lifetime values obtained in the absence and in the presence of trehalose show that the presence of the disaccharide affects the SUV/HSA binding interactions (Figure 2, open symbols) at both low and high [lipid]/[HSA] ratios. In the low regime, the disaccharide decreases the initial quenching observed for both types of vesicles. Trehalose has been shown to have lipid membrane associative properties[37] and to H-bond directly to the phosphate groups of phospholipids.[38] At low lipid concentration, the relative amount of trehalose is larger and we suggest that a larger number of sugar molecules bind the liposome surface, thus hindering HSA from depleting, and binding, individual lipid molecules from the vesicles. Consequently, the Trp quenching is not as efficient as that in the absence of trehalose. At higher [lipid]/[HSA] ratios, in the case of DMPC/DMPG vesicles, trehalose dampens the lifetime increase. This effect on protein−SUV interactions is expected if our electrostatically driven binding interpretation is valid: indeed, a trehalose-coated HSA would result in less binding of the negatively charged SUV, as observed. The ability of trehalose to coat the protein is due to the H-bonding ability of its alcoholic hydroxyl groups, which can act as donors, and to its hydrogens, which can act as acceptors.[39] Further, a recent molecular dynamics study has shown that the internal dynamics of proteins embedded in a trehalose matrix are strongly affected by this external matrix, thus severely hindering the capacity of the protein to undergo conformational changes.[40] This phenomenon could explain the less drastic lifetime changes observed in the presence of the disaccharide: necessarily, if the dynamics of the protein are restrained, so would the motion of the Trp indole and its capacity to increase or decrease its contact with potential quenchers.

As for the DMPC SUVs, we propose that trehalose, by its coating effect (on either the protein or the vesicles), hinders vesicle penetration by HSA, thus resulting in a higher fluorescence signal relative to the case without trehalose. In fact, the Trp lifetime data (Figure 2, open squares) are similar to the value of the pure HSA sample and thus are suggestive of no binding.

Effect of HSA and Trehalose on Aging. The relatively broad distribution curves and the large aggregation rates observed in the case of the neutral DMPC liposome systems do not allow firm conclusions concerning the DMPC liposome−HSA and/or trehalose interactions.

The results of the dynamic light scattering experiments performed on the DMPC/DMPG liposome−HSA system (Figure 3A and B) are in agreement with our earlier DSC measurements.[17] The ∼5 nm shift of the distribution functions toward larger sizes in the presence of HSA is indicative of the binding of HSA to the liposome surface. Besides the size, the aging process of the liposomes is also affected by HSA. We explain the more pronounced aggregation of DMPC/DMPG liposome−HSA complexes (Figure 3B), by the decreased repulsion of the negatively

(33) Zborowski, J. L.; Roerdink, F.; Scherpov, G. *Biochim. Biophys. Acta* **1977**, *497*, 183−191.
(34) Dimitrovaa, M. N.; Matsumuraa, H.; Dimitrovab, A.; Neitchevb, V. Z. *Int. J. Biol. Macromol.* **2000**, *27*, 187−194.
(35) Connor, J.; Pak, C. H.; Zwaal, R. F. A.; Schroit, A. J. *J. Biol. Chem.* **1992**, *267*, 19412−19417.
(36) Young, L.; Jernigan, B. L.; Covell, D. G. *Protein Sci.* **1994**, *3*, 717−729.
(37) Zhang, P.; Klymachyov, A. N.; Brown, S.; Ellington, J. G.; Grandinetti, P. J. *Solid State Nucl. Magn. Res.* **1998**, *12*, 221−225.
(38) Crowe, L. M. *Comp. Biochem. Physiol. A* **2002**, *131*, 505−513.
(39) Durvasula, R. V.; Huang, C. H. *Biochim. Biophys. Acta* **1999**, *1417*, 111−121.
(40) Cottone, G.; Cordone, L.; Ciccotti, G. *Biophys. J.* **2001**, *80*, 931−938.

charged surfaces of the vesicles as a result of their being covered by HSA molecules.

From the time dependence of the size distribution functions of the DMPC/DMPG liposomes in the absence and in the presence of trehalose (Figure 3A and C, respectively), we conclude that the disaccharide has a definite stabilizing effect on the liposomes also in the aqueous phase, even at the relatively low concentration used in our experiments. We attribute the increased homogeneity and the reduced aggregation rate of liposomes prepared in the presence of trehalose (Figure 3C) to H-bond formation between the PG headgroups and the sugar,[39] which results in steric hindrance.[41] The distribution curves shown in Figure 3D are consistent with trehalose also affecting liposome−HSA interaction. Although the first DMPC/DMPG liposome−HSA species formed in solution are not stable even in the presence of the sugar, the larger adducts developing during the first 3 days show a remarkable stability compared to the case without trehalose. From the change of the particle size distribution, we conclude that trehalose stabilizes the liposome−HSA complex as a larger aggregate consisting of a few individual liposome−HSA adducts.

Conclusion. In this work, we show that nonbond interactions play a decisive role in lipid−protein recognition. Experiments using charged and neutral SUVs combined with molecular-level insights obtained from modeling show that intricate modulation of favorable hydrophobic, electrostatic, and charge contacts can rank among the main determinants of the associative mechanisms. Further, this work confirms the ability of trehalose to significantly affect protein−lipid interactions as well as its stabilizing action. Our insights are in good agreement with the view arguing that the key to protein−protein association resides in the subtle interplay of the hydrophobic effect and polar interactions and that a favorable electrostatic interaction requires hydrophobic atoms to work cooperatively with hydrophilic ones.[42] Finally, we note that the correlation established between hydrophobic clusters on protein surfaces and the binding sites of their cofactors suggests that similar mechanisms may be involved in lipid−protein recognition.

Acknowledgment. The authors are grateful to G. Kellogg (Virginia Commonwealth University) for providing HINT version 2.3, to B. Honig (Columbia University) for the Grasp package, and to K. Módos for the MEM analysis program used to treat the dynamic light scattering data. The assistance of R. Markács and E. Bányai in sample preparation is highly appreciated. The authors also acknowledge the Hungarian Government's National Information Infrastructure Development Program (NIIFP) for providing computing time on the IIF parallel supercomputing environment, and support from Hungarian Grants ETT 228/2000 and OTKA 032117 (J.F.) and from the NATO Science Program (M.L.).

LA026166Q

(41) Lasic, D. D. *Liposomes from physics to applications*; Elsevier: Amsterdam, 1993; pp 263−310.

(42) Xu, D.; Suo, L.; Nussinov, R. *J. Mol. Biol.* **1997**, *265*, 68−84.